INFECTION AND IMMUNITY, Sept. 2003, p. 5266–5272 Vol. 71, No. 9
0019-9567/03/$08.00+0 DOI: 10.1128/IAI.71.9.5266–5272.2003


# SWR Mice Are Highly Susceptible to Pulmonary Infection with *Mycobacterium tuberculosis*

Oliver C. Turner,[1] Robert G. Keefe,[1] Isamu Sugawara,[2] Hiroyuki Yamada,[2] and Ian M. Orme[1]*

*Department of Microbiology, Immunology and Pathology, Colorado State University, Fort Collins, Colorado 80523,[1] and The Research Institute of Tuberculosis, Matsuyama, Kiyose, Tokyo, Japan[2]*

Received 3 January 2003/Returned for modification 18 February 2003/Accepted 5 June 2003

**Inbred mice differ in their abilities to control the growth of *Mycobacterium tuberculosis* in the lung and can as a result be regarded as either resistant or susceptible strains. In this study we report that the SWR mouse is both highly susceptible and in addition appears incapable of establishing a characteristic state of chronic disease after low-dose aerosol infection. In comparison to C57BL/6 mice, SWR mice were unable to contain the bacterial load in the lungs, resulting in progressive fatal disease. Histologic analysis of the lung tissue revealed evidence of a florid inflammatory cell response in the SWR mice leading to degeneration and necrosis and consolidation of a large percentage of the lung surface area. Digestion of infected lungs and analysis by flow cytometry demonstrated an initially similar but eventually higher number of lymphocytes accumulating in the SWR mice. Additionally, in contrast to the C57BL/6 mice, SWR mice had a significantly lower percentage of CD4 T cells in the lungs showing evidence of proliferation and positive intracellular staining for gamma interferon during the first two months of infection, and a lower percentage of both CD4 and CD8T cells exhibiting differentiation to an effector/memory phenotype during the first month of infection. We propose that further investigation of the SWR mouse may provide a new animal model for immunocompetent individuals apparently unable to effectively control the growth of *M. tuberculosis* in the lung.**

It is generally thought that most people exposed to *Mycobacterium tuberculosis* kill the organism by means of innate mechanisms and never develop disease. In those that do, the majority contain the bacterial load at low levels, establishing a form of chronic or latent disease in which there is a risk of reactivation at a later date, whereas the minority develop progressive disease and associated pneumonia which is fatal unless treated. The expression of this resistance is known to be further influenced by several host factors, including age, ethnicity, malnutrition, and concurrent disease (2–5, 11, 15), which may modulate the ability of the host to contain the primary infection and control the severity of the progressive disease.

To date, all immunocompetent inbred mouse strains studied in the low-dose-aerosol infection model are apparently able to contain the growth of the bacilli and establish a state of chronic disease. However, in the case of several strains, such as DBA/2, CBA/J, and A/J, etc., this control is relatively transient and fatal regrowth or reactivation disease then occurs about 150 days later (30). In contrast, mice bred on the C57 background develop this event very much more slowly, living approximately twice as long. This has been extensively described elsewhere (10, 19–21, 23), and as a result of these differences the former group of mice can be regarded as susceptible strains and C57 mice can be regarded as a resistant strain.

In this study we present evidence for a third category based upon observations made using the SWR strain of mouse, which appears to be incapable of establishing a state of chronic disease after aerosol infection. This study shows that whereas C57BL/6 mice expressed an expected long survival time, an ability to stabilize pulmonary bacterial growth, and a multifocal granulomatous inflammation characterized by aggregates of lymphocytes admixed with epithelioid macrophages, infected SWR mice exhibited reduced survival time, progressive bacterial growth, and severe pathology. Lesions were exemplified by a diffuse granulomatous pneumonia dominated by large epithelioid and foamy macrophages, multifocal necrosis and neutrophil accumulation, and scant aggregates of lymphocytes. Many of the SWR mice had crystalloid inclusions within lung macrophages, never seen in the C57BL/6 mice. SWR mice had more lymphocytes within the lung as the infection progressed, but a lower percentage had an activation-memory phenotype, fewer were proliferating, and fewer could be identified as $CD4^+$ gamma interferon (IFN-γ)-positive lymphocytes. Accordingly, the SWR mouse may provide a new animal model of pulmonary tuberculosis in which the infection is progressive and fatal.

## MATERIALS AND METHODS

**Mice.** Specific-pathogen-free, female C57BL/6 and SWR mice 6 to 8 weeks old were purchased from the Jackson Laboratories (Bar Harbor, Maine). Infected and uninfected control mice were maintained in a biosafety-level-3 facility at Colorado State University. All animals had free access to water and standard mouse chow. The specific-pathogen-free nature of the mouse colonies was demonstrated by testing sentinel animals. These were shown to be negative for 12 known mouse pathogens. In each experiment, four or five animals were used at each time point.

**Bacteria and infection.** *M. tuberculosis* strain Erdman (TMCC #107) was grown from low-passage-number seed lots in Proskauer-Beck liquid medium containing 0.02% Tween 80 to mid-log phase and then aliquoted and frozen at −70°C until use. Mice were infected via the aerosol route with a low dose of bacteria. Briefly, the nebulizer compartment of a Middlebrook airborne infection apparatus (Glas-col, Terre Haute, Ind.) was filled with 5 ml of $H_2O$ containing a suspension of bacteria, resulting in delivery of approximately 50 to 100 bacteria per lung during a 30-min exposure.

**Enumeration of bacteria.** At the times indicated, mice were euthanized by carbon dioxide asphyxiation. Lungs were aseptically removed from the thoracic

* Corresponding author. Mailing address: Department of Microbiology, Immunology and Pathology, Fort Collins, CO 80523. Phone: (970) 491-5777. Fax: (970) 491-5125. E-mail: iorme@lamar.colostate.edu.

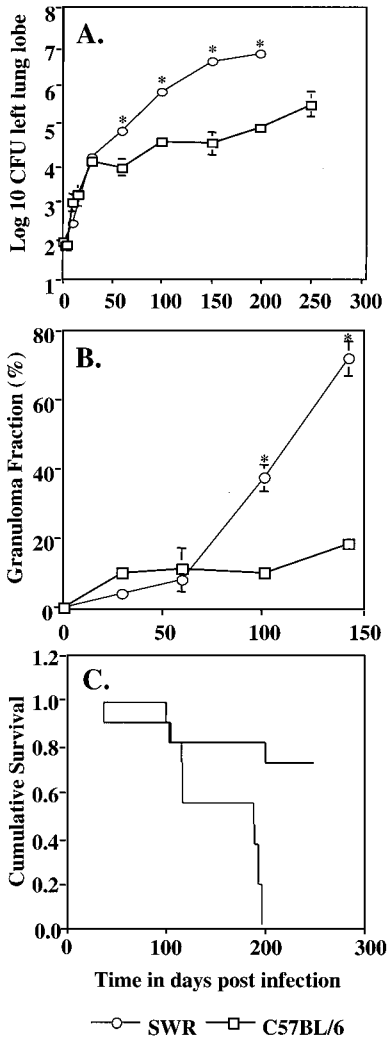


FIG. 1. (A) Bacterial growth curves in the lungs of mice infected with *M. tuberculosis.* (B) Granuloma fraction in the lungs of SWR and C57BL/6 (B6) mice after low-dose aerosol infection. (C) Cumulative survival curves. Statistically significant differences between strains ($P < 0.05$) are indicated (*). Survival curves are significantly different by the Kaplan-Meier method. Data are representative of two (B) or three (A) experiments or a combination of two (C) experiments ($n = 11$).

cavity, and the number of viable bacteria present was assessed by plating serial dilutions of left lung lobe homogenates onto Middlebrook 7H11 nutrient agar. After 3 weeks of incubation at 37°C in humidified air, bacterial colonies for each dilution were counted with a dissecting microscope (magnification, ×4). The data are representative of three experiments and are expressed as the $\log_{10}$ value of the mean number of CFU counted, with standard error of the mean indicated by vertical bars.

**Gross lesion assessment.** At each time point, an appraisal of gross lesions within the lung and thorax was made. All animals showing signs of distress were euthanized and, along with those that died unexpectedly, were necropsied. Cumulative survival curves were generated.

**Histology.** The lungs were removed from the thoracic cavity either as the entire organ or as individual lobes. The right cranial lung lobe, or all lung lobes, from each mouse were slowly infused with and then submerged in 10% neutral buffered formalin for a minimum of 72 h. Tissues were prepared routinely and sectioned for light microscopy with lobe orientation designed to allow the maximum surface area of each lobe to be seen. Consecutive sections were stained with hematoxylin and eosin, by the Ziehl-Neelsen method for the detection of acid-fast bacilli, and with Masson's Trichrome for detection of type IV collagen.

An assessment of all of the parenchymal and nonparenchymal tissue elements was performed in all sections. In each case the presence and distribution of inflammatory cell types was noted. This included macrophages, lymphocytes, multinucleated giant cells and granulocytes (neutrophils and eosinophils). The presence and distribution of acid fast bacilli and type IV collagen and necrosis was also noted. All tissue identification was masked and the order was randomized to preclude experimental group bias. Sections were examined at least three times to verify the reproducibility of the observations.

**Electron microscopy.** At each time point, the right accessory lung lobe was aseptically removed, diced into pieces no larger than 2 mm in diameter, and placed in a 4% formaldehyde–1.25% glutaraldehyde solution for a minimum of 72 h. The tissue was then processed for routine electron microscopic examination. Using a JEOL JEM-1200EX electron microscope with an accelerating voltage of 80 kV, multiple sections of lung from both strains were examined.

**Flow cytometric analysis of cell surface markers.** Lung lymphocytes from C57BL/6 and SWR mice were analyzed at day 30 and day 60 postinfection by flow cytometry. A single-cell suspension was prepared from lungs as described previously (12). Samples were stained for cell surface markers using rat anti-mouse monoclonal antibodies specific for mouse CD4 (L3T4 clone GK1.5,), CD8 (Ly-2 clone 53-6.7), CD25, CD44 (clone IM7), CD45RB (clone 16A), CD69 (clone H1.2F3), CD122, and OX40L. Appropriate isotype staining was also performed. All staining procedures were performed in RPMI 1640 without glutamine (Life Technologies, Rockville, Md.) with 0.1% azide. All antibodies were obtained from BD Pharmingen (San Diego, Calif.) as direct conjugates to fluorescein isothiocyanate (FITC), peridinin chlorophyll protein (PerCP), phycoerythin, or allophycocyanin. Acquisition was performed on a FACScalibur instrument (BD Immunocytometry Systems, San Jose, Calif.), and data were analyzed using CellQuest software (BD Immunocytometry Systems). Cells were gated for lymphocytes by their characteristic forward and side scatter profile, and 50,000 events in the lymphocyte gate per sample were counted. Markers are represented as a percentage of the cell population being analyzed.

**Assessment of T-cell proliferation by BrdU incorporation.** Mice infected with *M. tuberculosis* for 30 and 60 days were analyzed for BrdU incorporation using BD Pharmingen kit 2354KK. Mice were administered a solution of 5′-bromodeoxyuridine (BrdU) (Sigma-Aldrich, St. Louis, Mo.) at 0.8 mg/ml in sterile drinking water for 3 days prior to harvest of lungs. Single cell suspensions of lung tissue were harvested, resuspended at $5 \times 10^6$/ml in phosphate-buffered saline–0.1% azide, and stained for CD4-FITC and CD8-phycoerythin cell surface markers. The cells were fixed, permeabilized, and labeled with anti BrdU-FITC or isotype control antibodies. Analysis was performed by gating total lymphocytes by forward and side scatter.

**Assessment of intracellular IFN-γ production.** Single-cell suspensions of lungs at 30 and 60 days after aerosol infection were prepared and stained for intracellular IFN-γ. Briefly, cells were stimulated with anti-CD3 (clone 145-2C11, 0.1 μg/ml) and anti-CD28 (clone 37.51, 1 μg/ml) antibodies and 3 μM monensin (Sigma-Aldrich) for 4 h at 37°C. At the end of the stimulation period, cells were stained for CD4 and CD8, fixed, permeabilized, and stained for intracellular IFN-γ. Cells were resuspended at $5 \times 10^6$/ml in complete RPMI with 10% fetal

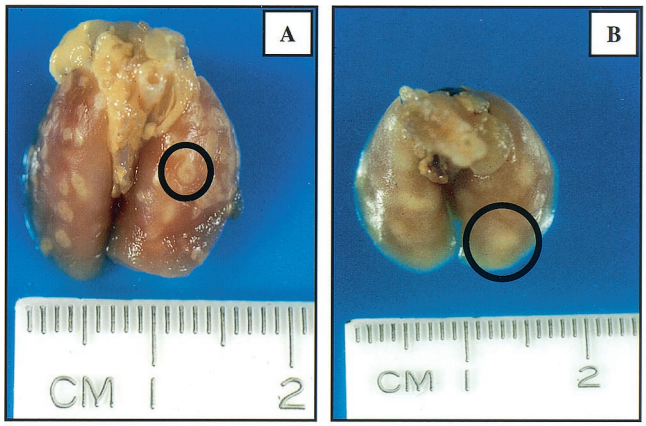


FIG. 2. Representative photographs of organs from C57BL/6 (A) and SWR (B) mice at 143 days after aerosol infection with *M. tuberculosis*. In each image, a typical granuloma is highlighted by a black circle. Note the distinct lesion in A and a more diffuse lesion in B. Changes are representative of three experiments.

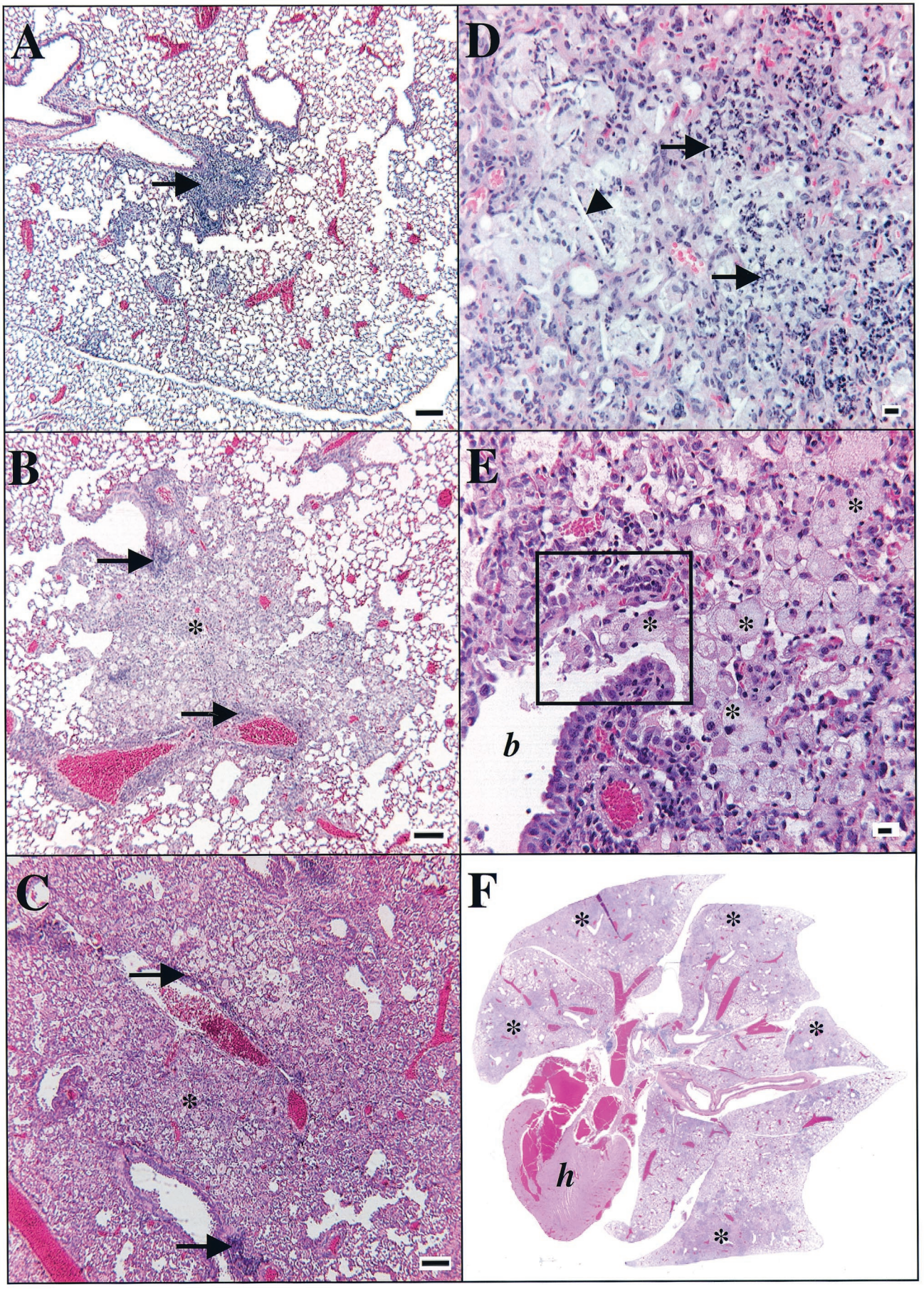
A
D
B
E
b
C
F
h

bovine serum. Analysis was performed by gating total lymphocytes by forward and side scatter and staining for CD4 or CD8.

**Photomicroscopy and morphometry.** Photomicroscopy was performed with an Olympus AH-2 microscope linked to a Sony SKC-DK5 digital camera and Adobe Photoshop 6.0 software. In an attempt to further classify the pulmonary lesions, the area of inflammation was calculated from each of the hematoxylin-and-eosin-stained histological slides. In brief, using Metamorph software (version 4.5r5; Universal Imaging Corporation), the perceived inflammatory area was determined by outlining the affected tissue on the captured images and expressing this as a percentage of the total area of the observed lung tissue. This percentage of affected tissue was termed the granuloma fraction (25, 26)

**Statistical analysis.** Statistical analysis was performed with the Sigma Stat 2 software program (SPSS Science, Chicago, Ill.). The one-way analysis of variance (ANOVA) and Student *t* test were used to analyze bacterial growth curve data. The Mann-Whitney rank sum test was used for the analysis of granuloma fraction, and Kaplan-Meier analysis was employed for cumulative survival. Statistical significance was taken as $P < 0.05$.

## RESULTS

**Course of *M. tuberculosis* infection in the lungs of C57BL/6 and SWR mice.** Over the course of the first 30 days postinfection the bacterial load in both strains increased at a similar rate. Thereafter, the bacterial load continued to increase progressively in the SWR mice (Fig. 1A). Assessment of the percentage of the lungs consolidated by the presence of the inflammation (granuloma fraction) showed that this reached a peak of almost 70% prior to the death of SWR mice compared to approximately 20% in the C57BL/6 mice at the same time (Fig. 1B). SWR mice showed a mean survival of approximately 150 days whereas the majority of the C57BL/6 mice lived until the experiment was terminated at 250 days (Fig. 1C).

**Gross appearance and histopathology.** Gross inspection of harvested lungs from SWR mice showed granulomas that had a poorly defined margin that often coalesced with adjacent lesions, in contrast to distinct, unitized, multifocal lesions seen in the C57BL/6 mice (Fig. 2) The results of microscopic analysis of C57BL/6 lungs was consistent with that previously described (23, 27). The significant findings in the SWR lungs are shown in Fig. 3 and 4. Figure 3 illustrates the progressive changes in pathology from a mild, mixed lymphocytic and histiocytic perivascular and peribronchiolar infiltrate at 30 days postinfection (Fig. 3A) to one that is characterized by extensive areas of large epithelioid and foamy macrophages admixed with granulocytes and punctuated by multiple areas of necrosis at the end stage of disease (Fig. 3B to F). Of note was the relative lack of lymphocytes at perivascular and peribronchiolar sites as the disease progresses and the preponderance of macrophages, many of which had a very large (diameter up to 50 μm) foamy and bizarre morphology. The presence of neutrophils and occasional eosinophils was also increasingly significant over time. Plasma cells and multinucleate giant cells were scattered to rare in the chronic lesions. Figure 4A and B illustrate the typical accumulation of bacilli within lesions and the scattered presence of type IV collagen within the inflammatory foci, respectively. Bacilli could be seen both within macrophages and extracellularly, admixed with cellular debris within the lumens of airways.

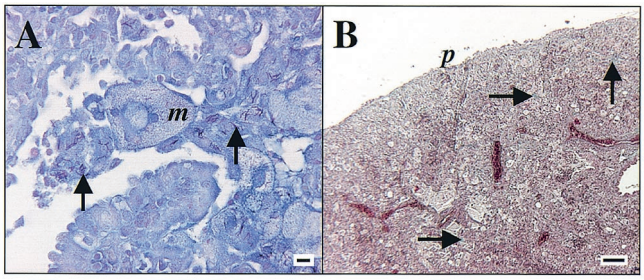


FIG. 4. Representative photomicrographs of lung stained for acid-fast bacilli (Ziehl-Neelsen method; bar = 10 μm) (A) and type IV collagen (Masson's Trichrome stain; bar = 100 μm) (B) in SWR mice at 143 days following low-dose-aerosol infection with *M. tuberculosis*. (A) The same area depicted in Fig. 3E is shown. Arrows, acid-fast bacilli and collagen; *m*, macrophage; *p*, pleura. Data are representative of three experiments.

**Ultrastructural changes.** As previously reported (31) many of the macrophages in the SWR mice had ultrastructural inclusions that were characterized as crystalloid, acicular, and electron dense (Fig. 5). No such inclusions were found in C57BL/6 mice.

**Flow cytometric analysis.** Analysis of CD4 and CD8 T cells entering the lungs is shown in Table 1. Cells were quantitated as activated ($CD69^{hi}$) or effector-memory ($CD44^{hi}$ $CD45RB^{lo}$). The percentages of CD4 T cells were similar in both mouse strains at days 30 and 60. The percentage of CD8 T cells in the SWR lungs, however, was less at day 30 but more at day 60 compared to C57BL/6. At both time points studied, greater than or equal to two-thirds of the CD4 cells in the C57BL/6 lungs expressed the effector-memory phenotype, whereas this was lower in the SWR lungs, rising from 33% on day 30 to 59% on day 60. In contrast CD4 T cells in both mouse strains had similar activation patterns at both time points, based on CD69 expression. The percentage of CD8 T cells within the effector-memory and activation sets was lower in SWR at day 30 but similar to C57BL/6 at day 60. Calculation of the total number of cells in the lungs (data not shown) showed that significantly more lymphocytes are present in the lungs of SWR mice by day 60, consistent with the histopathologic appearance of this organ.

**BrdU proliferation assay.** Cell proliferation in the lung was assessed by uptake of BrdU and flow cytometry (Fig. 6). The data show that more than three times as many CD4 cells in the

FIG. 3. Representative photomicrographs of lung from SWR mice after low-dose-aerosol infection with *M. tuberculosis.* (A) Thirty days postinfection. A small, focal lesion of perivascular lymphocyte and macrophage accumulation is shown (arrow). Bar = 100 μm. (B) Sixty days postinfection. A moderate-size lesion of perivascular and peribronchiolar lymphocyte accumulation (arrows) is shown with many macrophages (asterisk) filling adjacent alveoli. Bar = 100 μm. (C to E) One hundred ninety-nine days postinfection. (C) Severe, extensive inflammation with few perivascular lymphocytes (arrows) and extensive sheets of macrophages (asterisk) effacing the normal parenchyma are seen. Bar = 100 μm. (D) Neutrophils (arrows) and a cholesterol cleft (arrowhead) are seen. Bar = 10 μm. (E) Multiple foamy macrophages (asterisks) filling the lumen of a bronchiole (*b*) are seen. The area within the black box is depicted in Fig. 4A. (F) One hundred forty-three days postinfection. Organs are shown (magnification, ×1). *h* = heart. Note the extensive consolidation of all lobes (asterisks). Hematoxylin and eosin stain was used. Data are representative of three experiments.

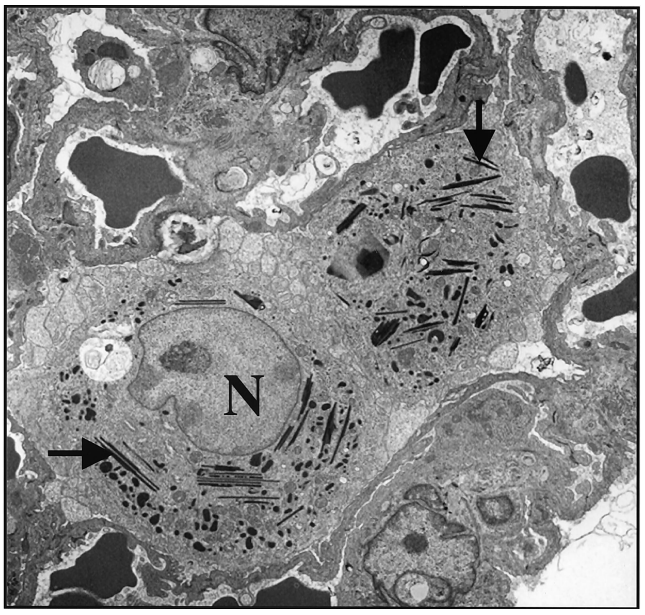


FIG. 5. Representative transmission electron micrographs of two alveolar macrophage from SWR mice at 99 days postinfection with a low-dose aerosol of *M. tuberculosis.* Multiple acicular, crystalline, osmiophilic intracytoplasmic inclusions are shown (arrows). N, nucleus (visible in only one of the macrophages). Magnification, ×2,000.

lungs of C57BL/6 mice were in a state of proliferation at day 30, whereas CD8-cell proliferation was low in both strains. Similar results were seen for day 60 of the infection (data not shown).

**Intracellular IFN-γ assay.** Lung cell digests were analyzed by flow cytometry to determine what percentage of CD4 and CD8 cells were expressing IFN-γ intracellularly (Fig. 7). Whereas this value was found to be about 15% of CD4 cells from C57BL/6 at both time points, only very low numbers of cells from SWR were positive. Interestingly, positive cells gated for CD8 from SWR mice were only marginally lower than those seen in C57BL/6 mice.

## DISCUSSION

The ability to establish a state of chronic disease is a common feature of inbred mouse strains studied to date. However, the immunological mechanisms controlling this event are still poorly understood (8), and as yet it is still unclear if the chronic stage is an active process in which continued expression of memory immunity is needed to restrain bacteria continually trying to divide and disseminate, or if it is more of a passive process in which the granulomatous process walls off foci of infected macrophages containing surviving bacilli that are in some sort of state of dormancy or latency.

Currently, there are data to support both the active and passive models. The predominance of the immunological data

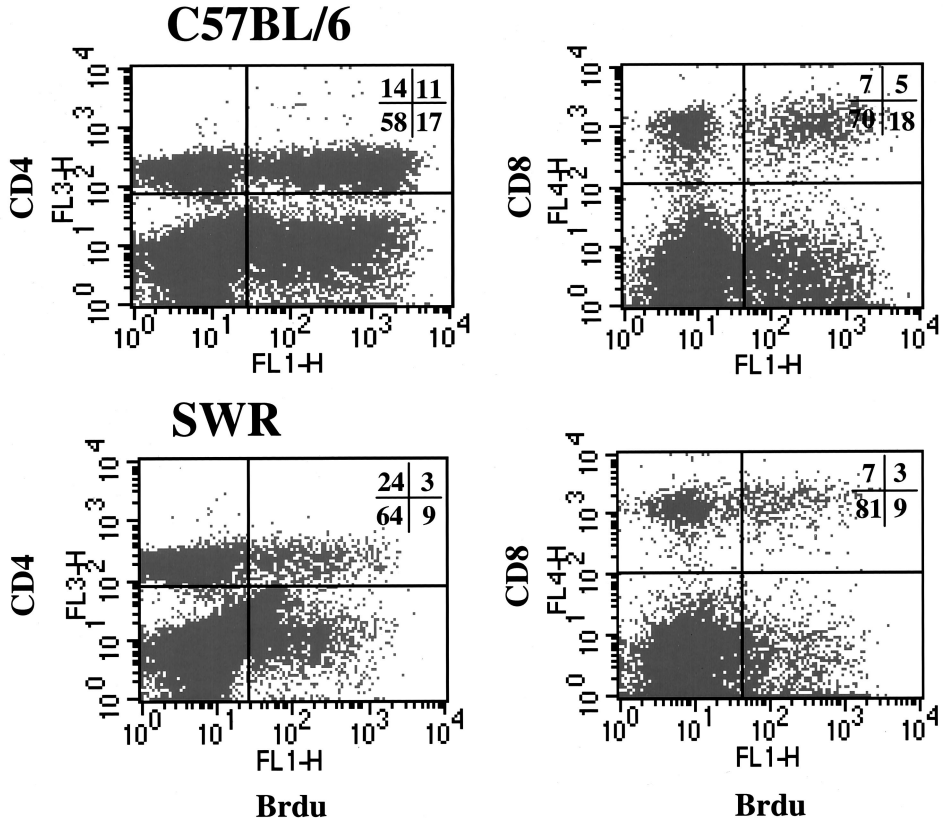


FIG. 6. Representative flow-cytometric dot plots of BrdU incorporation within $CD4^+$ and $CD8^+$ lung lymphocytes in C57BL/6 and SWR mice, 30 days postinfection with low-dose aerosol of *M. tuberculosis.* Percentages of total lymphocytes are represented.

TABLE 1. Flow cytometric analysis of pulmonary lymphocytes from C57BL/6 and SWR mice after a low-dose aerosol infection with *M. tuberculosis*[a]

| Day and cell | Result for hymphocytes from: | | | | | |
|---|---|---|---|---|---|---|
| | C57BL/6 mice | | | SWR mice | | |
| | % Lymphocytes (SD) | % Effector/memory[b] (SD) | % Activation[c] (SD) | % Lympocytes (SD) | % Effector/memory (SD) | % Activation (SD) |
| 30 | | | | | | |
| CD4 | 31 (2) | 76 (1) | 40 (5) | 33 (8) | 33 (9)[d] | 45 (9) |
| CD8 | 18 (3) | 51 (5) | 20 (1) | 13 (1)[d] | 36 (4)[d] | 13 (2)[d] |
| 60 | | | | | | |
| CD4 | 29 (3) | 66 (6) | 47 (8) | 32 (7) | 59 (6) | 43 (5) |
| CD8 | 13 (2) | 32 (7) | 35 (3) | 31 (2)[d] | 35 (5) | 32 (17) |

[a] Not shown: CD25, CD122, and OX40L (no differences between groups or time points).
[b] Effector/memory is defined as $CD44^{hi}/CD45RB^{lo\text{-}med}$ (CD45/CD45RB).
[c] Activation assessed by CD69 bright staining.
[d] Statistically significant difference for corresponding value in C57BL/6 by Student's *t* test ($P < 0.05$).

supports the former: prevention of the Th1 pathway prevents the emergence of the chronic state (6, 9, 28), and depression of CD4 immunity by human immunodeficiency virus infection triggers reactivation of tuberculosis (16). In the mouse model, a reduction in the expression of IFN-γ in the lungs as a result of the failure to adequately focus T cells into lung tissues may be a key factor in the breakdown of the chronic disease state in susceptible mouse strains (6, 9), and it has been shown in addition that a lack of CD8 cells during this period also favors breakdown (29). In contrast, studies at the genetic level tend to favor a latency hypothesis. Bacteria grown under hostile conditions in vitro tend to up-regulate stress and survival genes, and bacilli lacking the isocitrate lyase gene fail to persist in vivo (18). This of course is mainly a semantic debate and it is likely that both types of mechanisms are in fact involved (14, 24).

In the clinical setting, reactivation disease is a common cause of tuberculosis, and analysis of the course of events in mice resistant or susceptible to reactivation after initially establishing chronic disease is continuing. We report here that our observations of the SWR mouse strain may provide an additional opportunity. This mouse cannot establish a state of chronic disease, and may therefore serve as a new model of those individuals who are especially susceptible to tuberculosis despite the absence of secondary underlying causes.

Infection in the SWR causes a florid inflammatory response with very large numbers of mononuclear cells accumulating in the lungs. Despite this, however, the acquired specific response is depressed, and there is less proliferation. In addition, although the levels of CD4 and CD8 cell activation were generally similar in SWR and C57BL/6 mice (as measured by CD69, CD25, and OX40L levels), the level of intracellular IFN-γ production was consistently lower in SWR mice. These data thus suggest that there is not an activation defect per se but potential deficiencies in (i) antigen presentation, (ii) costimulatory activity of antigen presenting cells, or (iii) common signal transduction machinery such as NF-κB, allowing increased expression of CD69 and CD25 activation markers but depressing IFN-γ production or cell cycling. As a result the infection could not be contained, leading to the increased pathology and more rapid disease progression.

Poor antigen-presenting cell function might be associated with the intriguing observation that many macrophages in the lungs of SWR mice contain inclusion bodies (13, 31). How these arise is not known, but it is thought that they may represent eosinophil- or neutrophil-derived granules that have been phagocytosed (1, 22). These inclusions and the intense eosinophilic nature of the macrophage cytoplasm in some

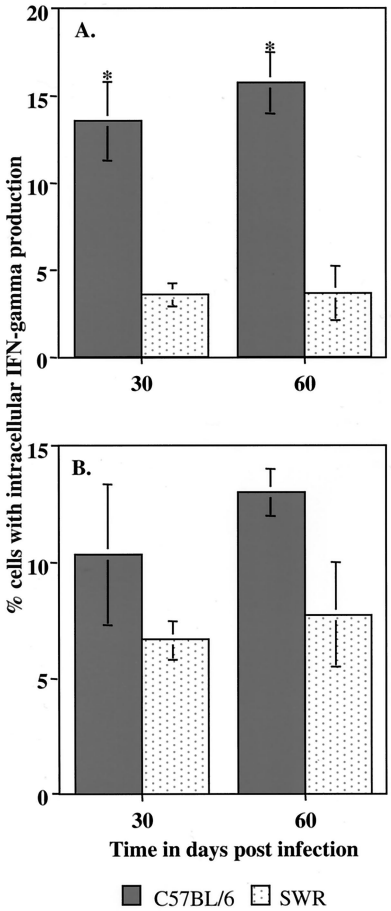


FIG. 7. Intracellular IFN-γ production in lung lymphocytes of C57BL/6 and SWR mice ([A] $CD4^+$; [B] $CD8^+$) following low-dose-aerosol infection with *M. tuberculosis.* Data are expressed as mean values ($n = 3$), with standard errors indicated with vertical bars. *, significant difference between values, using Student's *t* test ($P < 0.05$).

SWR lesions are very similar to those described in the idiopathic condition acidophilic macrophage pneumonia (22).

In fact, there may be multiple reasons underlying the heightened susceptibility of the SWR mouse. Lung digest studies revealed evidence of a delay in recruitment of effector T cells into the lungs, which could be explained in terms of a reduced early chemokine response, and/or poorer expression of adhesion and integrin molecules; these possibilities are currently under investigation. In addition, there is some limited information suggesting that SWR mice have poor NK cell activity. In the present study one interesting aspect of the histopathology was the perivascular cuffing but poor migration of lymphocytes out into the lung granuloma, which as a result consisted predominantly of macrophages. This observation is reminiscent of our previous observation with $\beta_2$-microglobulin gene-disrupted mice (7), which also lack NK cells and which show a similar histopathologic appearance. A recent study using class-Ia-KO mice makes a similar observation (32).

The degree of susceptibility of the SWR strain has some similarities to the I/St strain described elsewhere (17). In those studies, the I/St mouse was found to be highly susceptible to high-dose intravenous infection with *M. tuberculosis*. Those mice, like the SWR mice studied here, showed a significantly reduced expansion of CD4 cells expressing effector-memory cell phenotypes. In contrast, however, the I/St mice showed an increase in T-cell proliferation and reduced CD8-T-cell recruitment into the lungs, whereas in our study we observed the reverse. Thus, the I/St strain may provide an additional, useful model, but unfortunately unlike the SWR it is not widely available.

## ACKNOWLEDGMENTS

This work was supported by NIH grants AI-44072 and HL-55967.

## REFERENCES

1. **Ali, B. A., J. R. Shortland, and G. Hudson.** 1981. Origin of crystalloid inclusions in macrophages II: evidence for derivation from eosinophil granulocyte breakdown. Br. J. Exp. Pathol. **62:**662–668.
2. **Bellamy, R.** 2000. Identifying genetic susceptibility factors for tuberculosis in Africans: a combined approach using a candidate gene study and a genome-wide screen. Clin. Sci. (London) **98:**245–250.
3. **Bellamy, R., N. Beyers, K. P. McAdam, C. Ruwende, R. Gie, P. Samaai, D. Bester, M. Meyer, T. Corrah, M. Collin, D. R. Camidge, D. Wilkinson, E. Hoal-Van Helden, H. C. Whittle, W. Amos, P. van Helden, and A. V. Hill.** 2000. Genetic susceptibility to tuberculosis in Africans: a genome-wide scan. Proc. Natl. Acad. Sci. USA **97:**8005–8009.
4. **Bellamy, R., and A. V. Hill.** 1998. Genetic susceptibility to mycobacteria and other infectious pathogens in humans. Curr. Opin. Immunol. **10:**483–487.
5. **Bellamy, R., C. Ruwende, T. Corrah, K. P. McAdam, H. C. Whittle, and A. V. Hill.** 1998. Variations in the NRAMP1 gene and susceptibility to tuberculosis in West Africans. N. Engl. J. Med. **338:**640–644.
6. **Cooper, A. M., D. K. Dalton, T. A. Stewart, J. P. Griffin, D. G. Russell, and I. M. Orme.** 1993. Disseminated tuberculosis in interferon gamma gene-disrupted mice. J. Exp. Med. **178:**2243–2247.
7. **D'Souza, C. D., A. M. Cooper, A. A. Frank, S. Ehlers, J. Turner, A. Bendelac, and I. M. Orme.** 2000. A novel nonclassic beta2-microglobulin-restricted mechanism influencing early lymphocyte accumulation and subsequent resistance to tuberculosis in the lung. Am. J. Respir. Cell Mol. Biol. **23:**188–193.
8. **Flynn, J. L., and J. Chan.** 2001. Immunology of tuberculosis. Annu. Rev. Immunol. **19:**93–129.
9. **Flynn, J. L., J. Chan, K. J. Triebold, D. K. Dalton, T. A. Stewart, and B. R. Bloom.** 1993. An essential role for interferon gamma in resistance to *Mycobacterium tuberculosis* infection. J. Exp. Med. **178:**2249–2254.
10. **Flynn, J. L., M. M. Goldstein, K. J. Triebold, B. Koller, and B. R. Bloom.** 1992. Major histocompatibility complex class I-restricted T cells are required for resistance to Mycobacterium tuberculosis infection. Proc. Natl. Acad. Sci. USA **89:**12013–12017.
11. **Goldfeld, A. E., J. C. Delgado, S. Thim, M. V. Bozon, A. M. Uglialoro, D. Turbay, C. Cohen, and E. J. Yunis.** 1998. Association of an HLA-DQ allele with clinical tuberculosis. JAMA **279:**226–228.
12. **Gonzalez-Juarrero, M., O. C. Turner, J. Turner, P. Marietta, J. V. Brooks, and I. M. Orme.** 2001. Temporal and spatial arrangement of lymphocytes within lung granulomas induced by aerosol infection with *Mycobacterium tuberculosis*. Infect. Immun. **69:**1722–1728.
13. **Green, E. U.** 1942. On the occurrence of crystalline material in the lungs of normal and cancerous Swiss mice. Cancer Res. **2:**210–217.
14. **Honer zu Bentrup, K., and D. G. Russell.** 2001. Mycobacterial persistence: adaptation to a changing environment. Trends Microbiol. **9:**597–605.
15. **James, D. G., and A. Zumla.** 1999. The granulomatous disorders. Cambridge University Press, Cambridge, United Kingdom.
16. **Lawn, S. D., S. T. Butera, and T. M. Shinnick.** 2002. Tuberculosis unleashed: the impact of human immunodeficiency virus infection on the host granulomatous response to Mycobacterium tuberculosis. Microbes Infect. **4:**635–646.
17. **Lyadova, I. V., E. B. Eruslanov, S. V. Khaidukov, V. V. Yeremeev, K. B. Majorov, A. V. Pichugin, B. V. Nikonenko, T. K. Kondratieva, and A. S. Apt.** 2000. Comparative analysis of T lymphocytes recovered from the lungs of mice genetically susceptible, resistant, and hyperresistant to Mycobacterium tuberculosis-triggered disease. J. Immunol. **165:**5921–5931.
18. **McKinney, J. D., K. Honer zu Bentrup, E. J. Munoz-Elias, A. Miczak, B. Chen, W. T. Chan, D. Swenson, J. C. Sacchettini, W. R. Jacobs, Jr., and D. G. Russell.** 2000. Persistence of Mycobacterium tuberculosis in macrophages and mice requires the glyoxylate shunt enzyme isocitrate lyase. Nature **406:**735–738.
19. **Medina, E., and R. J. North.** 1996. Evidence inconsistent with a role for the Bcg gene (Nramp1) in resistance of mice to infection with virulent Mycobacterium tuberculosis. J. Exp. Med. **183:**1045–1051.
20. **Medina, E., B. J. Rogerson, and R. J. North.** 1996. The Nramp1 antimicrobial resistance gene segregates independently of resistance to virulent Mycobacterium tuberculosis. Immunology **88:**479–481.
21. **Medina, E., and R. J. North.** 1998. Resistance ranking of some common inbred mouse strains to Mycobacterium tuberculosis and relationship to major histocompatibility complex haplotype and Nramp1 genotype. Immunology **93:**270–274.
22. **Murray, A. B., and A. Luz.** 1990. Acidophilic macrophage pneumonia in laboratory mice. Vet. Pathol. **27:**274–281.
23. **Musa, S. A., Y. Kim, R. Hashim, G. Z. Wang, C. Dimmer, and D. W. Smith.** 1987. Response of inbred mice to aerosol challenge with *Mycobacterium tuberculosis*. Infect. Immun. **55:**1862–1866.
24. **Orme, M.** 2001. The latent tuberculosis bacillus (I'll let you know if I ever meet one). Int. J. Tuberc. Lung Dis. **5:**589–593.
25. **Orrell, J. M., S. J. Brett, J. Ivanyi, G. Coghill, A. Grant, and J. S. Beck.** 1991. Measurement of the tissue distribution of immunoperoxidase staining with polyclonal anti-BCG serum in lung granulomata of mice infected with Mycobacterium tuberculosis. J. Pathol. **164:**41–45.
26. **Orrell, J. M., S. J. Brett, J. Ivanyi, G. Coghill, A. Grant, and J. S. Beck.** 1992. Morphometric analysis of *Mycobacterium tuberculosis* infection in mice suggests a genetic influence on the generation of the granulomatous inflammatory response. J. Pathol. **166:**77–82.
27. **Rhoades, E. R., A. A. Frank, and I. M. Orme.** 1997. Progression of chronic pulmonary tuberculosis in mice aerogenically infected with virulent *Mycobacterium tuberculosis.* Tuber. Lung Dis. **78:**57–66.
28. **Saunders, B., A. Frank, I. Orme, and A. Cooper.** 2002. CD4 is required for the development of a protective granulomatous response to pulmonary tuberculosis. Cell. Immunol. **216:**65–72.
29. **Turner, J., C. D. D'Souza, J. E. Pearl, P. Marietta, M. Noel, A. A. Frank, R. Appelberg, I. M. Orme, and A. M. Cooper.** 2001. CD8- and CD95/95L-dependent mechanisms of resistance in mice with chronic pulmonary tuberculosis. Am. J. Respir. Cell Mol. Biol. **24:**203–209.
30. **Turner, J., M. Gonzalez-Juarrero, B. M. Saunders, J. V. Brooks, P. Marietta, D. L. Ellis, A. A. Frank, A. M. Cooper, and I. M. Orme.** 2001. Immunological basis for reactivation of tuberculosis in mice. Infect. Immun. **69:**3264–3270.
31. **Turner, O. C., Sugawara, H. Yamada, B. Cummings, and I. M. Orme.** 2001. Crystalloid inclusions in the cytoplasm of alveolar macrophages of the SWR/J mouse. A possible cause of susceptibility to mycobacterium tuberculosis? J. Submicrosc. Cytol. Pathol. **33:**217–219.
32. **Urdahl, K. B., D. Liggitt, and M. J. Bevan.** 2003. MHC Class-Ib restricted CD8 T cells accumulate in the lungs of *Mycobacterium tuberculosis*-infected mice but provide minimal protection. J. Immunol. **170:**1987–1994.

*Editor:* S. H. E. Kaufmann